CONCEPT

Concept of Utilizing Ionic Liquids for the Co-electroreduction of Carbon Dioxide and Nitrogen-containing Compounds

Saudagar Dongare[a,*], Oguz Kagan Coskun, Burcu Gurkan[b,*]

Department of Chemical and Biomolecular Engineering, Case Western Reserve University, Cleveland, Ohio, USA, 44106.

***E-mail:** [a] sbd54@case.edu; [b] beg23@case.edu

Abstract: Formation of C–N bonds through the electrochemical utilization of CO_2 and nitrogen containing compounds (N-compounds) is appealing for the purpose of converting waste and readily available sources or pollutants into value added chemicals at ambient conditions. Existing research predominantly explores these electrochemical reactions independently, often in aqueous electrolytes, leading to challenges associated with competitive hydrogen evolution reaction (HER), low product selectivity, and yield. Functional electrolytes such as those containing ionic liquids (ILs) present selective solubility to the solute reactants and present unique interactions with the electrode surface that can suppress the undesired side reaction HER while simultaneously co-catalyzing the conversion of CO_2 and N-compounds such as N_2, NO, NO_2, and NO_3. In this concept paper, we discuss how the microenvironment enabled by ILs can be leveraged to stabilize reaction intermediates at the electrode-electrolyte interface, thereby promoting C–N bond formation on an active electrode surface at reduced overpotential, with the case study of CO_2 and N-compounds co-catalysis to generate urea.

Introduction

With the global annual production of 184 million metric tons[1], urea is considered an important nitrogen source for the fertilizer industry. Presently, the production of urea is accomplished by the reaction of N_2 and H_2 to generate NH_3 by the Haber–Bosch process at high temperature and pressure (350–550 °C, 150–350 bar) in the first step, followed by the reaction of NH_3 and CO_2 under relatively milder reaction conditions (170–200 °C and 200–250 bar) in the second step. These sequential reactions are carried out for several cycles to increase the conversion efficiency since both N_2 and CO_2 molecules are extremely inert, with high dissociation energies of N≡N (941 kJ/mol)[2] and C=O (806 kJ/mol)[3]. Thus, current methods are energy-intensive, with production costs accounting for about 2% of annual global energy.[4] Recently, electrochemical urea synthesis has been reported as an alternative where the co-reduction of greenhouse gas CO_2 and naturally abundant N_2 under ambient conditions were achieved using a range of electrocatalysts including monometallics[5], bimetallic[6], oxides[7], and multi-component alloys[8]. However, the first electron transfer reactions to CO_2 and N_2 involving $CO_2^{\bullet-}$ and N_2H species still necessitate high overpotentials of −1.9 V and -1.4 V *vs.* reversible hydrogen electrode (RHE),[9] respectively. This results in HER side reaction in aqueous media and thereby limiting the urea production efficiency. Another factor contributing to low production rates is the low solubility of CO_2 and N_2 in the aqueous electrolyte. Therefore, the development of both the electrodes and suitable electrolytes simultaneously for the enhanced solubility and co-reduction of CO_2 and N_2 remain an unmet need.[10]

Research has shown that other nitrogen sources with lower dissociation energies than N_2 can be advantageous to address the high overpotential challenge such as nitrite, NO_2^- (207 kJ/mol)[7], nitrate, NO_3^- (204 kJ/mol)[2], and NO (607 kJ/mol)[5]; these species also demonstrate higher solubility in aqueous electrolytes than N_2. Furuya and colleagues[11] reported the electrosynthesis of urea by co-reduction of CO_2 and NO_3^-/NO_2^- using Cu-loaded gas-diffusion electrodes. They observed 37 % current efficiency for urea at -0.75 V *vs.* standard hydrogen electrode (SHE). Assuming a pH of 7, based on the use of 0.2 M $KHCO_3$, the reported potential corresponds to -0.33 V *vs.* RHE. The mechanism they proposed involved the formation of ammonia intermediate from nitrite, which then reacts with the in-situ formed CO on the electrode surface. Since this first study, many different strategies such as heteroatom doping,[12] controlling oxygen vacancy defects,[13] and surface engineering[14] by nanoalloys have been reported for the formation of C-N bond to selectively produce urea on a heterogenous catalyst as summarized in **Table 1**. For example, Chen et al.[15] developed PdCu alloy nanoparticles supported on TiO_2 nanosheets where they achieved overpotentials as low as − 0.40 V *vs.* RHE in a flow cell assembly, similar to Furuya and colleagues, despite their utilization of N_2.

Most of the aqueous based studies discuss the surface adsorbed $*NH_2$ and *COOH as key intermediates during the co-reduction of nitrogenous species and CO_2, respectively. Therefore, it is necessary that these intermediates are coupled at the interface an early stage of the mechanism to achieve an increased urea selectivity compared to the byproducts such as NH_3, CO, or HCOOH.[11] Despite the many advancements in catalyst development aimed at achieving suboptimal binding of key intermediates on various active sites, the process lacks a benchmark in terms of urea yield rate and selectivity for practical applications. Therefore, it is necessary to also engineer the electrolyte side to help stabilize reaction intermediates on the surface for C-N coupling. To this end, ionic liquids (ILs) and specifically those based on imidazolium cation have been reported to induce electric field effects on metal electrodes and act as co-catalysts or promoters for electrochemical reactions, particularly the CO_2 reduction.[16] Separately, the higher solubility of N_2 in ILs (up to 20 times higher), compared to aqueous electrolytes (only 0.66 mmol/L)[17], are reported to be the reason

for the enhanced N_2 electro-reduction to ammonia in the IL electrolytes.[18]

This article summarizes key insights from studies showcasing IL-assisted CO_2 and N_2 electrochemical reduction and present the concept of coupling these reactions for the specific case of urea electrosynthesis. Specifically, we hypothesize that the introduction of functional ions to electrolytes can enhance the solubility of nitrogenous compounds and CO_2 from low partial pressure gas streams such as flue gas, thereby facilitating improved mass transport of reactants and intermediates to active sites within electrode materials. Moreover, the unique microenvironment at the electrode-electrolyte interface created by the IL can be leveraged toward stabilizing reaction intermediates on catalytic active sites for enhanced catalyst efficiency and product selectivity. As ILs behave differently on surfaces, depending on the electrode material, it is also important to synergize the choice of the electrode with the specific IL electrolyte.[19]

Table 1. Catalysts for electrosynthesis of urea in aqueous electrolytes with a comparison to the only report to date with IL electrolytes for benchmarking in terms of type of reactants, applied potentials (V *vs.* RHE), current density (CD), yield rate, and Faradaic efficiency (FE). Differently than the aqueous electrolysis studies, the IL electrolyte work followed a sequential 2-stage process where amines were the N-source and O_2 reduction to H_2O_2 was an additional reaction.

Electrocatalyst	**Electrolyte**	**Reactant**	**Potential (V *vs.* RHE)**	**CD ($mA \cdot cm^{-2}$)**	**Yield rate ($mmol\ h^{-1}\ g^{-1}$)**	**FE_{urea} (%)**
Aqueous electrolytes						
$In(OH)_3$-S[20]	0.1 M KNO_3	NO_3^- + CO_2	-0.6	-2	8.53	53.4
InOOH[21]	0.1 M $KHCO_3$	N_2 + CO_2	-0.4	-1.2	9.8	51
Bi_2S_3/N-RGO[22]	0.1 M $KHCO_3$	N_2 + CO_2	-0.5	-0.75	4.4	7.5
MoP-(101)[23]	0.1 M $KHCO_3$	N_2 + CO_2	-0.3	-	0.2	36.5
ZnMn-N,Cl[24]	0.1 M $KHCO_3$	N_2 + CO_2	-0.3	-0.75	4.1	63.5
Zn NBs[5]	0.2 M $KHCO_3$	NO + CO_2	-0.9	-40	15.1	11.3
Cu–TiO_2–V_o[7]	0.2 M $KHCO_3$ + 0.02 M KNO_2	NO_2^- + CO_2	-0.4	-8	20.8	43.1
AuCu SANFs[25]	0.5 M $KHCO_3$ + 0.01 M KNO_2	NO_2^- + CO_2	-1.5	-20	64.7	24.7
PdCu/CBC[6]	0.05 M KNO_3	NO_3^- + CO_2	-0.5	-2	12.7	69.1
Pd_4Cu_1–$FeNi(OH)_2$[8]	0.1 M $KHCO_3$ + 0.1 M KNO_3	NO_3^- + CO_2	-0.5	-1.5	18.8	76.2
$CuWO_4$[26]	0.1 M KNO_3	NO_3^- + CO_2	-0.2	-1	1.5	70.1
Cu-GS-800[27]	0.1 M $KHCO_3$ + 0.1 M KNO_3	NO_3^- + CO_2	−0.9	−27	-	28
IL electrolytes						
Au plate[28]	[BMIM][NTf_2] (1^{st}) + Cyclohexylamine (2^{nd})	CO_2 + amine + O_2	-1.6 V *vs.* Fc^+/Fc	N/A	N/A	88
	[BMPyrr][NTf_2] (1^{st}) + Cyclohexylamine (2^{nd})	CO_2 + amine + O_2	-1.6 V *vs.* Fc^+/Fc	N/A	N/A	93

Electrocatalytic reduction of N_2 in ILs

There is a body of literature[29] devoted to understanding the solubility behavior of gases in ILs motivated by their potential applications in gas separations. Stevanovic and Gomes[17] investigated the solubility of CO_2, N_2O, C_2H_6, and N_2 in 1-butyl-1-methylpyrrolidinium tris(pentafluoroethyl) trifluorophosphate ([C_4mpyr][eFAP]) and trihexyl(tetradecyl)phosphonium tris(pentafluoroethyl) trifluorophosphate ([P_{66614}][eFAP]). Notably, they observed that N_2 exhibited a solubility level approximately one order of magnitude lower than other gases but still higher than in pure water. Expanding on this work, Gomes's group[30] explored ILs with partially fluorinated cations, revealing a positive correlation between the fluorine content in ILs and the solubility of CO_2 and N_2. More recently, MacFarlane and colleagues[31] examined the electrochemical NH_3 production over a nanostructured iron catalyst from N_2 in ambient air using the same ILs as electrolytes in comparison to a common IL, 1-hexyl-3-methylimidazolium bis(trifluoromethylsulfonyl)imide ([HMIM][NTf_2]. They reported the highest NH_3 selectivity was with [P_{66614}][eFAP] with 60% FE at around −0.8 V *vs.* NHE (equivalent to -1.5 V *vs.* Fc/Fc^+) over a nanostructured iron catalyst under ambient conditions followed by [C_4mpyr][eFAP] (FE=40%) and [HMIM][NTf_2] (FE=0.64%). This trend was consistent with the N_2 solubility in these ILs: 0.28 $mg \cdot g^{-1}$ ([P_{66614}][eFAP]), 0.20 $mg \cdot g^{-1}$ ([C_4mpyr][eFAP]), and <0.017 $mg \cdot g^{-1}$ ([HMIM][NTf_2]) at about 1 bar and 30 °C.[17] These solubilities correspond to Henry's law constants approximately in the range of 100-200 bar.

In a subsequent study, MacFarlane and colleagues[32] introduced a fluorinated co-solvent, 1H,1H,5H-octafluoropentyl-1,1,2,2-tetrafluoroethyl ether, to develop aprotic solvent-IL mixture electrolytes to simultaneously achieve high N_2 and regulated H^+ availability on an iron based electrode surface. They achieved 32% FE for NH_3 with a yield of 2.35×10^{-11} $mol \cdot s^{-1} \cdot cm^{-2}$, in comparison to 10^{-12} $mol \cdot s^{-1} \cdot cm^{-2}$ in the neat IL, [C_4mpyr][eFAP]. This study demonstrated the enhanced catalytic activity due to increased N_2 solubility and the improved stabilization of the first reduced $*N_2H$ intermediate by the fluorinated IL electrolyte. Further, Lopez and colleagues[33] performed density functional theory (DFT) calculations to gain mechanistic insight on the role of hydrogen bonding interaction for N_2RR at Ru(0001) surface modified by [C_4mpyr][eFAP]. The hydrogen bonding between the fluorous anion (-CF_2) and the N_2H intermediate stabilizes this intermediate on the surface for multi-electron transfers, thus increasing catalytic activity and boost selectivity toward NH_3. More recently, Wei et al.[34] studied the behavior of [C_4mpyr][eFAP] IL on P-doped MoS_2 nanospheres. They observed suppression of HER due to hydrophobic IL electrolyte and its stronger interaction with the surface that prevents water approaching to the electrode. They reported 69% FE for NO to NH_3 conversion at -0.6 V *vs.* RHE.

Separately, in search of stable non-aqueous electrolytes, Hoang-Long et al.[35] demonstrated that a concentrated solution of imide-based lithium salt (2 M Li[NTf_2] in tetrahydrofuran, 3.5 ppm H_2O) promotes N_2RR over a Ni wire electrode for a minimum of 96 hours tested. Consistent NH_3 yield rates, reaching 223 $nmol/s/cm^2$, with nearly 100% NH_3 conversion efficiency, were achieved. This study further highlights the importance of ionic assembly at the electrode surface modulated by Li^+ with the [NTf_2] anion in the presence of the non-aqueous electrolytes, thus preventing electrolyte decomposition while enabling stable N_2RR.

Saudagar Dongare received his master's degree from LIT Nagpur, India, in 2016, and his Ph.D. from Thapar Institute, Patiala, India, in 2021. Since then, he has been working as a postdoctoral researcher at Case Western Reserve University, Cleveland, USA, under the supervision of Prof. Burcu Gurkan. His current research interests involve interfacial characterizations of functional solvents in CO_2 capture and electrochemical conversion processes.

Oguz Kagan Coskun is a Ph.D. student at Case Western Reserve University under the supervision of Prof. Burcu Gurkan. He completed his B.S. in Metallurgical and Materials Engineering and M.Sc. in Materials Science and Engineering at Istanbul Technical University focusing on molten salt electrolysis. His research interests involve electrode–electrolyte interfaces, electrocatalyst materials, ionic liquid electrolytes, and analytical and computational electrochemistry.

Burcu E. Gurkan is a Professor of Chemical and Biomolecular Engineering Department at Case Western Reserve University. Her research focuses on the physical properties and reactivity in deep eutectic solvents and ionic liquids for applications in separations, energy storage, and conversion. She is the Deputy Director of BEES2 (Breakthrough Electrolytes for Energy Storage Systems)—a Department of Energy Frontier Research Center (EFRC) and a Key Researcher in 4C (Center for Closing the Carbon Cycle) EFRC where she leads the effort in developing structured electrolytes for electrochemical processes for flow batteries and CO_2 conversion, respectively.

Electrocatalytic reduction of CO_2 in ILs

The electrochemical CO_2RR in aqueous electrolytes faces challenges due to its energetic inefficiency, necessitating large overpotentials for the initial electron transfer to convert linear CO_2 into bent $CO_2^{\bullet-}$. This high overpotential often leads to competition from HER, reducing the Faradaic efficiency for producing reduced CO_2 products. Additionally, the low solubility of CO_2 in aqueous solutions exacerbates these challenges.

ILs are known for their high CO_2 solubility (Henyr's law constants in the orders of 20 to 60 bar);[36] however, beyond increased solubility, ILs offer co-catalytic effects and inhibit parasitic reactions like HER. Among the various types of ILs, imidazolium-based ones have attracted the most interest in CO_2RR. The earliest report by Rosen et al.[16c] using 18 mol% 1-ethyl-3-methyl-imidazolium tetrafluoroborate ([EMIM][BF_4]) aqueous solution reported 96% FE for CO over silver with a lower overpotential (200 mV more positive compared to the aqueous electrolyte without the IL). Besides lowering the energy barrier for reactions, the presence of ILs in non-aqueous electrolytes were also reported to influence the reaction mechanisms; for example, the generation of CO instead of the expected oxalate on Pb surface as reported by Sun et al.[37] Other studies have delved into the performance of alternative catalysts, yielding noteworthy findings. For instance, MoS_2 and Nb-doped MoS_2 exhibit a higher turnover frequency for CO compared to Ag nanoparticles in an Im-based IL-water mixture.[38] It is important to highlight the role of electrode material in IL-mediated CO_2RR, as demonstrated by Tanner et al.[39], where a series of electrode materials was studied including Ag, Pt, Au, Sn and Pb and the earliest onset potential was observed on Ag electrode. The authors concluded the co-catalytic effect observed through earlier onset potentials to be Ag specific.

Regarding the role of ILs in catalyzing CO_2RR, initial reports focused on $[EMIM]^+$ claimed that the co-catalytic affect is a result of interaction between the cation and the CO_2 yielding a complex (i.e., carboxylate).[40] This proposed mechanism later challenged by other researchers in the field who propose that the complex formation is not the origin of co-catalytic effect but the hydrogen bonding interactions[41] and ordering in the double layer structure of the interface leading to reduced entropy, hence the reduced overpotentials.[42] In fact, various in-situ interface probing techniques, such as sum frequency generation spectroscopy, surface tunnelling microscopy, or surface-enhanced Raman spectroscopy, indicate potential-dependent transitions in the ordering of ILs near the electrode surface.[16a] Consequently, these structural changes, induced mainly by negative potentials during reduction can impact the electric field strength and help stabilize intermediates like $CO_2^{\bullet-}$.[43]

The range of ILs capable of co-catalyzing the CO_2RR extends beyond imidazolium-based ILs. Pyrazolium-based ILs have also been reported as stable co-catalysts where 500 mV decrease in the overpotential with 100% FE for CO were obtained.[44] Fully substituted pyrazolium cations demonstrate favorable performance in CO_2RR, inhibiting the inactive pyrazolium-CO_2 adduct formation, similar to the carboxylate formation in the case of imidazolium-ILs, thus increasing CO_2 utilization. In another study conducted by Vasilyev et al.[45], guadinium-based ILs were systematically assessed as co-catalysts for the CO_2RR in comparison to imidazolium, pyrrolidinium and pyrazolium based ILs, with an aim to identify the factors influencing their activity. The researchers found that the accessibility of the charge on the IL cation plays a crucial role in facilitating interactions with surface-bound $CO_2^{\bullet-}$ species. Moreover, they observed that these interactions are enhanced when the charge distribution on the cation is localized. These identified descriptors were then used to explain the trends observed among various IL co-catalysts in the CO_2RR, where imidazolium, pyrrolidinium, and pyrazolium based ILs exhibited comparable activity levels, surpassing guadinium-ILs. Furthermore, non-substituted ILs performed better than the substituted ILs. Based on these findings, the authors conclude that the optimal IL cation should feature a highly localized charge with minimal steric hindrance, promoting efficient interactions with $CO_2^{\bullet-}$ and resulting in enhanced catalytic activity.

Early investigations of IL-mediated CO_2 reduction studies primarily focused on physisorbing ILs, where the CO_2 and IL components do not chemically interact. However, emergence of functionalized ILs introduces a more dynamic interface, extending beyond dissolved neutral CO_2 to adducts formed between CO_2 and the IL components such as carboxylate and carbamate species.[46] The more complex and dynamic interfacial ordering created by these species presents chemical processes like hydrogen transfer to the electrode surface and among IL components in addition to electron transfer reactions between the electrode and the electrolyte.[47] For example, an imidazolium based IL with 2-cyanopyrrolide anion ($[2\text{-CNpyr}]^-$) chemisorbs CO_2 (about 5 mmol of CO_2 per gram of IL at 1 bar and 25 °C) and the spontaneous chemical reaction generates native hydrogen bond donor upon proton transfer from imidazolium to the anion in addition to cation-CO_2 and anion-CO_2 complexes.[46, 48] The formation of the native hydrogen bond donor helps tune the hydrogen bonding network within the double layer and the catalytic activity towards higher value CO_2RR products.[16a]

In summary, ILs are shown to tune the interfacial electric field and create advantageous hydrogen bonding networks besides suppressing HER and promoting selectivity towards certain products by structural design. While the product generation yields remain low for practical solutions, the existing literature findings merit further research in co-electrolysis approaches with ILs for making chemicals and fuels using renewable electricity to adapt to decarbonization efforts for a sustainable future.

Co-catalysis of CO_2 and N-compounds with IL electrolytes

The overall urea electrosynthesis reaction from co-catalysis of CO_2 and N-compounds (reactions 1-4 below) involves simultaneous multi-proton coupling and multi-electron transfer processes with various reaction intermediates, as shown in **Figure 1**.

$N_2 + CO_2 + 6H^+ + 6e^- = CO(NH_2)_2 + H_2O$ (1)

$2NO_3^- + CO_2 + 18H^+ + 16e^- = CO(NH_2)_2 + 7H_2O$ (2)

$2NO_2^- + CO_2 + 14H^+ + 12e^- = CO(NH_2)_2 + 5H_2O$ (3)

$2NO + CO_2 + 10H^+ + 10e^- = CO(NH_2)_2 + 3H_2O$ (4)

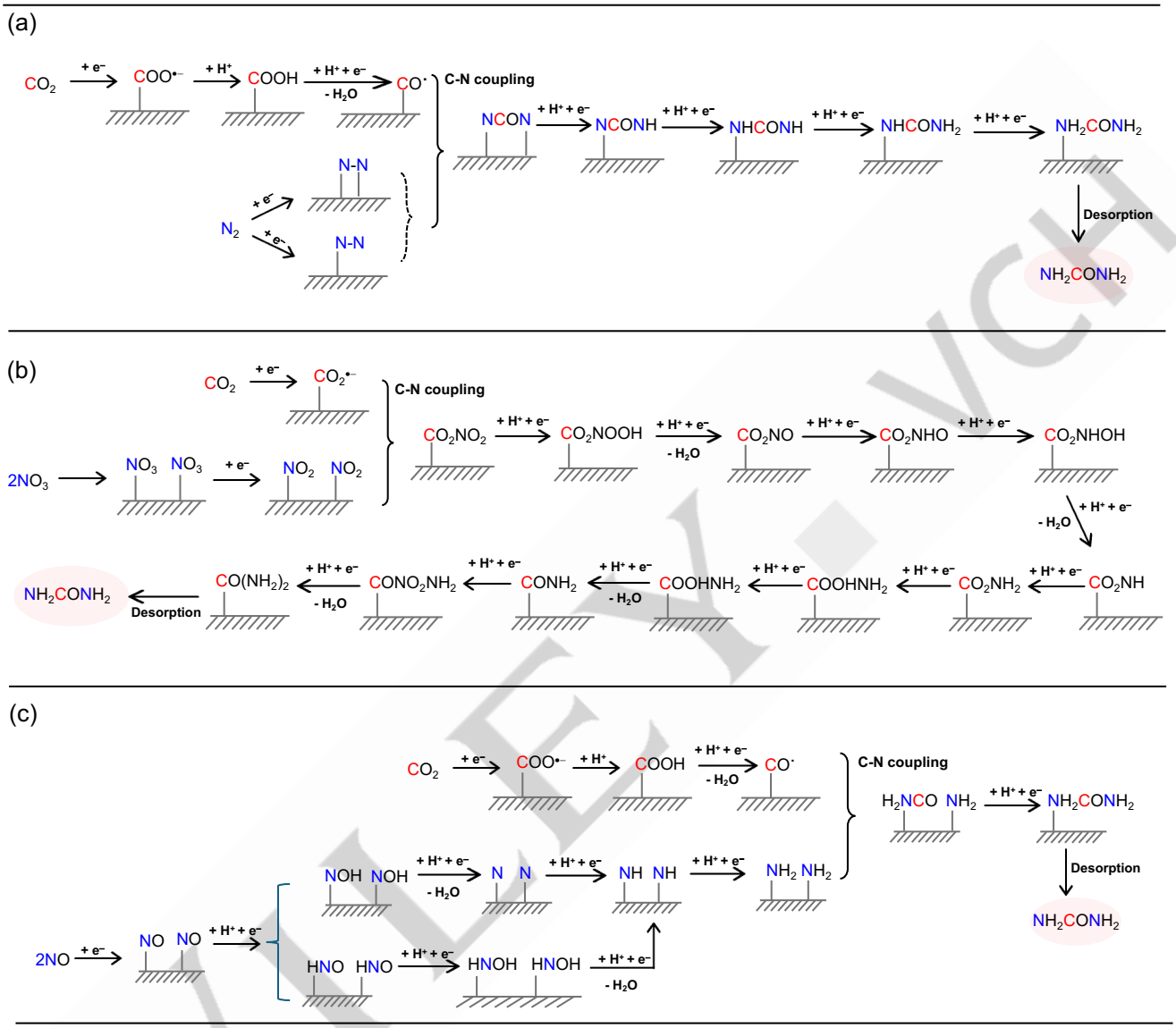

Figure 1. The possible reaction pathway of urea synthesis from co-reduction of CO_2 and N_2 (a) and NO_3^- (b), and NO (c). The reduction of NO_2^- follows a similar reaction pathway as shown in panel (b).

The reactions of interest to the co-reduction of CO_2 and N-compounds (eqns. 1-4) typically involve three steps. First step is the co-activation step that is followed by adsorption on catalytic active sites to form intermediates. Second step is the coupling of the reduction intermediates to form C–N bonds. Finally, the third step is the hydrogenation of key reaction intermediates to generate urea.[23] Current research has been confined to only a few theoretical calculations[49] and in situ spectroscopic investigations, including synchrotron radiation-Fourier transform infrared spectroscopy (SR- FTIR)[13a], sum frequency generation spectroscopy (SFG)[49a], and, Raman spectroscopy[50], especially in aqueous electrolytes, where various key intermediates were detected. In the case of N_2 as the N source, the C–N coupling reaction proceeds through the interactions between the surface adsorbed *N=N* and *CO to form *NHCONH followed by additional protonation step to form *$NHCONH_2$ intermediate,[51] as illustrated in **Figure 1a**. However, in the case of CO_2 and NO_x co-electrolysis, coupling proceeds through *NO_2 and *CO_2 or *NH_2 and *CO intermediates to form *CO_2NO_2 [13] and *$CONH_2$[7] as shown in **Figures 1b** and **1c,** respectively. The type of electrode material, its morphology, and composition greatly influence the reaction pathways. It has been reported that the C-N coupling steps and protonation of key reaction intermediates during the co-electrolysis reactions are thermodynamically unfavorable (ΔG >0.40 eV),[52] leading to poor urea synthesis specifically on Cu surface. It is also possible that other undesired hydrogenation

reactions occur with these reaction intermediates in a similar reaction environment, including the hydrogenation of *NH_2 to form NH_3 and the hydrogenation of *$CONH_2$ to produce formamide.[53] Furthermore, adsorbed HCHO* (CO_2RR intermediate) quickly undergoes nucleophilic attack by NH_2OH (N_2RR intermediate), yielding formaldoxime, which is further electrochemically reduced to n-methylhydroxylamine and then to methylamine[54] and ethylamine[55] on cobalt β-tetraaminophthalocyanine/carbon nanotubes (CoPc-NH_2/CNT) and CuO nanoparticles/carbon fiber, respectively. The occurrence of these undesired side reactions decreases urea selectivity. Therefore, it is necessary to control the hydron bonding network at the interface to mitigate such undesired reactions. Other problems include the low solubility of CO_2 and N-containing compounds, low diffusion rates of reactants to the electrode surface, HER, low urea yield rate, and separation of products.[10c] Therefore, based on our understanding of the field and the current literature, we propose that utilizing IL as an electrolyte could improve the urea selectivity and yield rates as further rationalized in the consecutive sections.

a. Solubility of CO_2 and N-compounds in ILs

The solubility of CO_2 and nitrogen oxides (NO_x), including N_2O, NO, and NO_2, is limited in conventional solvents, and sometimes they react with solvents (as is the case with amines), causing electrolyte degradation after repeated use and long exposure during the conversion process.[56] Further, limited solubility of reactants will induce mass transfer limitations during electrolysis at higher current densities. Researchers have utilized membrane electrode assembly and gas diffusion electrodes in flow cells with a gas phase CO_2 feed to overcome solubility limits, as these setups create a triple-phase boundary where gaseous reactants is in contact with an electrolyte close to the electrocatalytic surface. However, these types of electrodes are known to become less hydrophobic during electrolysis at highly negative potentials because of electrowetting of carbon sites under an applied electrical field,[57] chemical degradation,[58] and salt precipitation.[59] Such configurations also require the use of pure gas streams coupled with high surface area electrocatalysts to achieve the desired product selectivity and current densities,[60] thereby adding to the cost burden of catalyst synthesis, gas separation, and compression.

In recent years, ILs have been proposed as an alternative for the capture and separation of CO_2 and NO_x compounds because of their stability and high capacities. Generally, NO_x are polar molecules, which can potentially be absorbed by polar solvents according to the law of similarity and miscibility. ILs are generally considered as 'very polar' solvents due to the presence of charged ions in their structure.[61] For example, Anthony et al.[29b] reported the first solubility data of N_2O in 1-butyl-3-methylimidazolium bis(trifluoromethylsulfonyl)imide ([BMIM][Tf_2N]) at three temperatures (283.15 K, 298.15 K, and 323.15 K) and pressures up to 1.3 MPa. They showed that the solubilities of N_2O and CO_2 are essentially the same (on a mole fraction basis) in [BMIM][Tf2N] and have significantly higher solubility than other hydrocarbons (C_2H_4, C_2H_6) and oxygen. Further, imidazolium[30] and phosphonium[62]-based ILs with highly fluorinated anions were reported to have remarkable N_2 solubility. It has been reported that adding fluorinated functional groups to either the cation or the anion increases N_2 and CO_2 solubility, which can be explained by the rigidity of the fluorinated chains leading to a larger free volume.[62-63] Similarly, functionalizing ILs with amino, carboxylate, alkoxide, phenolate, azolate functional group enables chemisorption with high CO_2 uptake capacities even at low CO_2 partial pressure. Some example structures of ILs that demonstrated high CO_2 and N_2/NO_x uptake capacity are shown in **Figure 2.**

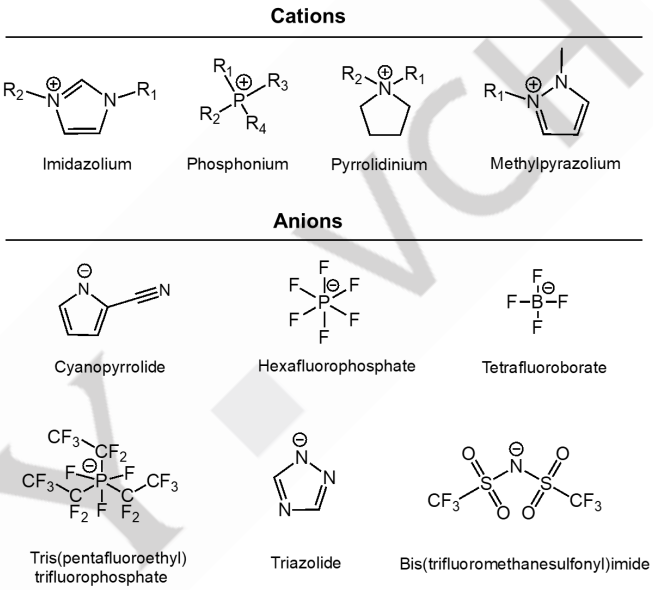

Figure 2. Common cation and anion structures of IL those were reported for high CO_2 and N_2/NO_x uptake capacity.

These ILs can be utilized as functional electrolytes solubilizing large quantities of reactants during the co-electrolysis process, which can further eliminate the need of complex reactor configuration and reactant separation and further purifications. In electrosynthesis using ILs as the reaction media or the co-catalyst, a special attention should be paid to ensure IL itself is stable and not contributing to side reactions. To confirm the source of carbon and nitrogen in C-N coupling reactions, particularly with ILs containing N- and C- based ions, isotope labeling of reactants (^{15}N and ^{13}C) would be helpful. It is important to ensure IL is stable under the conversion reaction conditions and that the observed products are not derived from the degradation of the IL or the electrolyte itself, especially under high reduction overpotentials. Another concern may arise regarding the conversion of the captured reactants as it may require additional energy to break the covalent bonds, if formed, between the IL and the solutes at the electrode surface. Further research is needed to understand the solute-solvent interactions in parallel to those of solute-electrode in chemically complexing systems undergoing electron transfer reactions such as the case of simultaneous CO_2RR and N_2RR.

b. Hydrophobicity at the interface

In the practical applications, flue gas typically contains 8% to 20% moisture along with other impurities. The presence of moisture and undesired impurities (e.g., halides) in the electrolyte can cause side reactions such as hydrogenation of intermediates in competition to the urea electrosynthesis. To address this issue, hydrophobic ILs such as those containing fluoro moieties and long chain alkyl substituents can be utilized to control the water activity at the electrode surface. Studies by Seddon et al.[65] and Cao et al.[66], have examined the impact of IL structural components on water sorption from the atmosphere. They found that the hydrophobicity of IL is decreased with increasing alkyl chain length of the cation. Further, they reported that the anion of the IL plays a more significant role in tuning hydrophobicity compared to the cation. The water sorption capacity among the imidazolium ILs with varied anions followed the order of acetate($[Ac]^-$) > trifluoroacetate ($[TFA]^-$) > nitrate ($[NO_3]^-$) > trifluorometahnesulphonate ($[TFO]^-$) > tetrafluoroborate ($[BF_4]^-$) > bis(trifluoromethylsulfonyl)imide ($[Tf_2N]^-$) > cholate ($[CHO]^-$) > hexafluorophosphate ($[PF_6]^-$).[66]

ILs with functional amines and aprotic heterocyclic compounds are also shown to enhance CO_2 solubility[67] and reactivity at the electrode-electrolyte interface for CO_2RR.[16a, 47] As an example, Feng et al.[64] reported hydrophobic IL functionalized with aprotic heterocylic amine, trihexyltetradecylphosphonium 1,2,4 triazolide ($[P_{66614}]$[124-Trz]) coated on Ni foam and used as free-standing electrocatalyst during CO_2RR. The $[P_{66614}]$[124-Trz] itself has very high CO_2 uptake capacity of 0.91 mol CO_2/mol IL versus 0.0006 mol CO_2/mol H_2O at atmospheric temperature and pressure. They reported that coating $[P_{66614}]$[124-Trz] on Ni foam helped to offer high CO_2 concentration around the electrode/electrolyte interface and suppress the HER, achieving 63% FE for CO in 0.5 M $KHCO_3$ electrolyte. Further, tuning the interfacial hydrophobicity using fluorinated IL is also reported to be effective strategy to increase the N_2 solubility and achieve high NH_3 selectivity during N_2RR.[62]

c. Stabilization of reaction intermediates

Key reaction intermediates shown in **Figure 1** need to be stabilized on the surface to facilitate C-N bond formation and improve the current density and selectivity for urea production. The modification of the interfacial electric field is recognized as an efficient strategy to stabilize the reaction intermediates. This can be achieved by either morphology-induced[68] or cation-induced[69] interfacial electric field effects. The cation-induced electric field can be achieved more effectively by utilizing IL electrolytes, which can change the concentration as a proxy for altering ionic correlations under applied potentials, thereby impacting the magnitude of electric fields at interfaces. For example, presence of $[EMIM][BF_4]$ at intermediate concentrations (0.125-0.9 M) facilitate thin double layers[16b] with an ordered structure of [EMIM] cations.[42] As a result, the local electric field at the interface is enhanced to further stabilize the critical reaction intermediates for multi-proton/electron transfers to achieve desired product. Ummireddi et al.[70] studied series of pyrazolium and imidazolium ILs to examine the IL-induced electric field on stabilizing the $CO_2^{\bullet-}$ intermediate. Based on their Bader charge analysis by DFT, they reported that 1-butyl-3-methylimidazolium ([BMIM]) cation with a higher electron donating ability (-1.17e on N) than 1-butyl-2-methylpyrazolium ([BMPyra]) cation (-0.75e on N) better stabilizes $CO_2^{\bullet-}$ on the electrode surface during CO_2RR. More recently, the CO_2 reactive IL 1-ethyl-3-methylimidazolium pyrrole-2-carbonitrile ([EMIM][2-CNpyr]) is also reported to modulate the interaction between the intermediates and the Cu electrode surface, thereby creating a unique microenvironment at the electrode-electrolyte interface for multi-carbon products.[16a]

d. Rational design of electrocatalyst

The advances in the electrolyte design and formulation, especially with ILs including mostly organic ions cannot be a disconnected effort from the heterogenous catalyst and the electrode design. To date, significant progress has been made in design and construction of active sites on catalyst surface/subsurface including the regulation of surface morphology,[5, 25] heteroatom doping,[22] and, composition[26] to improve and maintain urea selectivity. For example, developing catalyst materials with multiple adjacent active sites at an appropriate distance showed increased C–N coupling efficiency as reported by Zhao et al.[26]. They synthesized Cu–W bimetallic oxide ($CuWO_4$) electrocatalyst for the co-electrolysis of NO_3^- and CO_2, where Cu site is active for CO_2 reduction and the neighboring W site promotes the activation of nitrogenous species, which favors the coupling step. Through in-situ Raman, Differential Electrochemical Mass Spectrometry, and computational analysis, they confirmed that the high adsorption ability of *CO and $*NO_2$ intermediates on the alternating bimetallic W/Cu sites in $CuWO_4$ enhances the C–N coupling and reduces the potential barrier, resulting in 70% FE for urea at -0.2 V *vs.* RHE. In addition, several emerging classes of catalysts, such as dual single-atom catalysts,[71] enzyme-mimicking electrocatalysts,[72] and metal–organic frameworks,[73] also deserve attention and are potential candidates for C–N coupling reactions.

In complement to catalyst design, pulsed-potential electrolysis technique[74] is reported to facilitate mass transport of reactants and catalyst reconstruction, thereby revealing more active facets to leverage C-N bond formation. Recently, Gerke et al.[75] reported the pulsed-potential electrolysis to mediate nitrate transport during co-reduction of CO_2 and NO_3^-. They reported that the anodic and cathodic pulsing control adsorption of interfacial species, achieving 42% FE for urea at cathodic potentials of -0.4 V *vs.* RHE (t_c = 1 s) and anodic potential of 0.2 V *vs.* RHE (t_a = 0.2 s) over polycrystalline Au electrode and CO_2 saturated aqueous electrolyte (0.1 M KNO_3 + 0.1 M KHCO).

Several review articles have been published on covering catalyst design strategies for urea electrosynthesis with high selectivity and stability. For practical applications, it is also necessary to maintain long-term stability of such electrocatalysts; IL microenvironment could help to achieve this goal because of its formation of unique microenvironment. While ILs compare favorably compared to aqueous electrolytes in terms of their electrochemical stability window, their potential surface

interactions and possible side reactions need to be understood in detail.

Summary and Outlook

The electrochemical co-reduction of CO_2 and N-compounds, including N_2, NO, NO_2^-, and, $NO_3^-$for urea synthesis has attracted significant attention owing to its environment friendliness. Although electrosynthesis of urea is an active research area, the practical application is still a long way to go due to some significant obstacles, such as a relatively low solubility of CO_2 and N-compounds in traditional solvents, poor urea selectivity, competitive side reactions, and ambiguous C–N coupling reaction mechanisms. To some extent, the introduction of ILs in the electrolyte media has been demonstrated to be a viable strategy to improve the selectivity of CO_2RR and N-compound reduction reactions when studied separately. Here, we discuss the concept of co-electrolysis of CO_2 and N-compounds in IL based electrolytes with potential advantageous of high solubilities, better stabilization of key reaction intermediates, and suppression of the side reactions like HER, for promoting the desired product selectivity. Designing ILs with increased hydrophobicity and regulated hydrogen bonding network can promote C-N bond formation when combined with bimetallic electrodes. However, optimizing IL structure for maximized solubility of reactants or specific electric field or hydrogen bonding effects may not be sufficient for achieving industrially relevant selectivity and high yields of urea. Further research is needed to understand the mechanism and energetics of different C-N coupling reactions in ILs, including two-gas molecular reaction (CO_2+N_2 and CO_2+NO) and gas-liquid co-reaction (CO_2+NO_2 and CO_2+NO_3). Further, it is critical to understand the specific IL-electrode interactions with spectroscopic studies as well as the hydrodynamic and kinetic conditions in the electrochemical cell in order to develop appropriate pulsing techniques or cell arrangements for electrochemical synthesis.

Acknowledgements

This study was funded by an NSF CAREER award (no. 2045111) from the Division of Chemical, Bioengineering, Environmental and Transport Systems (CBET), Interfacial Engineering, and Electrochemical System.

Conflict of interest

The authors declare no conflict of interest.

Keywords: • Electrocatalytic C−N coupling • Electrolysis • Environmental chemistry • Ionic liquid • Urea

[1] International Fertilizer Industry Association. (February 13, Production of urea worldwide from 2009 to 2022 (in million metric tons) [Graph]. In Statista. Retrieved June 04, 2024, from https://www.statista.com/statistics/1287028/global-urea-production/.

[2] H. Xu, Y. Ma, J. Chen, W.-x. Zhang, J. Yang, *Chemical Society Reviews* **2022**, *51*, 2710-2758.

[3] S. Zhang, Q. Fan, R. Xia, T. J. Meyer, *Accounts of Chemical Research* **2020**, *53*, 255-264.

[4] Q. Wu, C. Dai, F. Meng, Y. Jiao, Z. J. Xu, *Nature Communications* **2024**, *15*, 1095.

[5] Y. Huang, R. Yang, C. Wang, N. Meng, Y. Shi, Y. Yu, B. Zhang, *ACS Energy Letters* **2022**, *7*, 284-291.

[6] S. Zhang, J. Geng, Z. Zhao, M. Jin, W. Li, Y. Ye, K. Li, G. Wang, Y. Zhang, H. Yin, H. Zhang, H. Zhao, *EES Catalysis* **2023**, *1*, 45-53.

[7] N. Cao, Y. Quan, A. Guan, C. Yang, Y. Ji, L. Zhang, G. Zheng, *Journal of Colloid and Interface Science* **2020**, *577*, 109-114.

[8] M. Xu, F. Wu, Y. Zhang, Y. Yao, G. Zhu, X. Li, L. Chen, G. Jia, X. Wu, Y. Huang, P. Gao, W. Ye, *Nature Communications* **2023**, *14*, 6994.

[9] E. Tayyebi, Y. Abghoui, E. Skúlason, *ACS Catalysis* **2019**, *9*, 11137-11145.

[10] aC. Chen, N. He, S. Wang, *Small Science* **2021**, *1*, 2100070; bY. Wang, D. Chen, C. Chen, S. Wang, *Accounts of Chemical Research* **2024**, *57*, 247-256; cC. Yang, Z. Li, J. Xu, Y. Jiang, W. Zhu, *Green Chemistry* **2024**, *26*, 4908-4933.

[11] M. Shibata, K. Yoshida, N. Furuya, *Journal of Electroanalytical Chemistry* **1995**, *387*, 143-145.

[12] X. Liu, P. V. Kumar, Q. Chen, L. Zhao, F. Ye, X. Ma, D. Liu, X. Chen, L. Dai, C. Hu, *Applied Catalysis B: Environmental* **2022**, *316*, 121618.

[13] aC. Lv, C. Lee, L. Zhong, H. Liu, J. Liu, L. Yang, C. Yan, W. Yu, H. H. Hng, Z. Qi, L. Song, S. Li, K. P. Loh, Q. Yan, G. Yu, *ACS Nano* **2022**, *16*, 8213-8222; bN. Meng, Y. Huang, Y. Liu, Y. Yu, B. Zhang, *Cell Reports Physical Science* **2021**, *2*, 100697.

[14] H. Wang, Y. Jiang, S. Li, F. Gou, X. Liu, Y. Jiang, W. Luo, W. Shen, R. He, M. Li, *Applied Catalysis B: Environmental* **2022**, *318*, 121819.

[15] C. Chen, X. Zhu, X. Wen, Y. Zhou, L. Zhou, H. Li, L. Tao, Q. Li, S. Du, T. Liu, D. Yan, C. Xie, Y. Zou, Y. Wang, R. Chen, J. Huo, Y. Li, J. Cheng, H. Su, X. Zhao, W. Cheng, Q. Liu, H. Lin, J. Luo, J. Chen, M. Dong, K. Cheng, C. Li, S. Wang, *Nature Chemistry* **2020**, *12*, 717-724.

[16] aO. K. Coskun, S. Dongare, B. Doherty, A. Klemm, M. Tuckerman, B. Gurkan, *Angewandte Chemie International Edition* **2024**, *63*, e202312163; bB. Liu, W. Guo, M. A. Gebbie, *ACS Catalysis* **2022**, *12*, 9706-9716; cB. A. Rosen, A. Salehi-Khojin, M. R. Thorson, W. Zhu, D. T. Whipple, P. J. A. Kenis, R. I. Masel, *Science* **2011**, *334*, 643-644.

[17] S. Stevanovic, M. F. Costa Gomes, *The Journal of Chemical Thermodynamics* **2013**, *59*, 65-71.

[18] Y. Tian, Y. Liu, H. Wang, L. Liu, W. Hu, *ACS Sustainable Chemistry & Engineering* **2022**, *10*, 4345-4358.

[19] aO. K. Coskun, M. Muñoz, S. Dongare, W. Dean, B. E. Gurkan, *Langmuir* **2024**, *40*, 3283-3300; bS. Dongare, O. K. Coskun, E. Cagli, J. S. Stanley, A. Q. Mir, R. S. Brower, J. M. Velázquez, J. Y. Yang, R. L. Sacci, B. Gurkan, *Langmuir* **2024**, *40*, 9426-9438; cW. Dean, D. Penley, Y.-Y. Lee, R. Ghahremani, S. Dongare, B. Gurkan, *The Journal of Physical Chemistry C* **2022**, *126*, 14598-14610; dW. Dean, J. Klein, B. Gurkan, *Journal of The Electrochemical Society* **2021**, *168*, 026503.

[20] C. Lv, L. Zhong, H. Liu, Z. Fang, C. Yan, M. Chen, Y. Kong, C. Lee, D. Liu, S. Li, J. Liu, L. Song, G. Chen, Q. Yan, G. Yu, *Nature Sustainability* **2021**, *4*, 868-876.

[21] M. Yuan, H. Zhang, Y. Xu, R. Liu, R. Wang, T. Zhao, J. Zhang, Z. Liu, H. He, C. Yang, S. Zhang, G. Zhang, *Chem Catalysis* **2022**, *2*, 309-320.

[22] P. Xing, S. Wei, Y. Zhang, X. Chen, L. Dai, Y. Wang, *ACS Applied Materials & Interfaces* **2023**, *15*, 22101-22111.

[23] D. Jiao, Y. Dong, X. Cui, Q. Cai, C. R. Cabrera, J. Zhao, Z. Chen, *Journal of Materials Chemistry A* **2023**, *11*, 232-240.

[24] X. Zhang, X. Zhu, S. Bo, C. Chen, K. Cheng, J. Zheng, S. Li, X. Tu, W. Chen, C. Xie, X. Wei, D. Wang, Y. Liu, P. Chen, S. P. Jiang, Y. Li, Q. Liu, C. Li, S. Wang, *Angewandte Chemie International Edition* **2023**, *62*, e202305447.

[25] S. Liu, S. Yin, Z. Wang, Y. Xu, X. Li, L. Wang, H. Wang, *Cell Reports Physical Science* **2022**, *3*, 100869.

[26] Y. Zhao, Y. Ding, W. Li, C. Liu, Y. Li, Z. Zhao, Y. Shan, F. Li, L. Sun, F. Li, *Nature Communications* **2023**, *14*, 4491.

[27] J. Leverett, T. Tran-Phu, J. A. Yuwono, P. Kumar, C. Kim, Q. Zhai, C. Han, J. Qu, J. Cairney, A. N. Simonov, R. K. Hocking, L. Dai, R. Daiyan, R. Amal, *Advanced Energy Materials* **2022**, *12*, 2201500.

[28] E. Witherspoon, P. Ling, W. Winchester, Q. Zhao, A. Ibrahim, K. E. Riley, Z. Wang, *ACS Omega* **2022**, *7*, 42828-42834.

[29] aJ. L. Anderson, J. K. Dixon, J. F. Brennecke, *Accounts of Chemical Research* **2007**, *40*, 1208-1216; bJ. L. Anthony, J. L. Anderson, E. J. Maginn, J. F. Brennecke, *The Journal of Physical Chemistry B* **2005**, *109*, 6366-6374.

[30] D. Almantariotis, A. S. Pensado, H. Q. N. Gunaratne, C. Hardacre, A. A. H. Pádua, J. Y. Coxam, M. F. Costa Gomes, *The Journal of Physical Chemistry B* **2017**, *121*, 426-436.

[31] F. Zhou, L. M. Azofra, M. Ali, M. Kar, A. N. Simonov, C. McDonnell-Worth, C. Sun, X. Zhang, D. R. MacFarlane, *Energy & Environmental Science* **2017**, *10*, 2516-2520.

[32] B. H. R. Suryanto, C. S. M. Kang, D. Wang, C. Xiao, F. Zhou, L. M. Azofra, L. Cavallo, X. Zhang, D. R. MacFarlane, *ACS Energy Letters* **2018**, *3*, 1219-1224.

[33] M. A. Ortuño, O. Hollóczki, B. Kirchner, N. López, *The Journal of Physical Chemistry Letters* **2019**, *10*, 513-517.

[34] T. Wei, H. Bao, X. Wang, S. Zhang, Q. Liu, J. Luo, X. Liu, *ChemCatChem* **2023**, *15*, e202201411.

[35] H.-L. Du, M. Chatti, R. Y. Hodgetts, P. V. Cherepanov, C. K. Nguyen, K. Matuszek, D. R. MacFarlane, A. N. Simonov, *Nature* **2022**, *609*, 722-727.

[36] C. Cadena, J. L. Anthony, J. K. Shah, T. I. Morrow, J. F. Brennecke, E. J. Maginn, *Journal of the American Chemical Society* **2004**, *126*, 5300-5308.

[37] L. Sun, G. K. Ramesha, P. V. Kamat, J. F. Brennecke, *Langmuir* **2014**, *30*, 6302-6308.

[38] P. Abbasi, M. Asadi, C. Liu, S. Sharifi-Asl, B. Sayahpour, A. Behranginia, P. Zapol, R. Shahbazian-Yassar, L. A. Curtiss, A. Salehi-Khojin, *ACS Nano* **2017**, *11*, 453-460.

[39] E. E. L. Tanner, C. Batchelor-McAuley, R. G. Compton, *The Journal of Physical Chemistry C* **2016**, *120*, 26442-26447.

[40] B. A. Rosen, J. L. Haan, P. Mukherjee, B. Braunschweig, W. Zhu, A. Salehi-Khojin, D. D. Dlott, R. I. Masel, *The Journal of Physical Chemistry C* **2012**, *116*, 15307-15312.

[41] G. P. S. Lau, M. Schreier, D. Vasilyev, R. Scopelliti, M. Grätzel, P. J. Dyson, *Journal of the American Chemical Society* **2016**, *138*, 7820-7823.

[42] S. Noh, Y. J. Cho, G. Zhang, M. Schreier, *Journal of the American Chemical Society* **2023**, *145*, 27657-27663.

[43] L. D. Chen, M. Urushihara, K. Chan, J. K. Nørskov, *ACS Catalysis* **2016**, *6*, 7133-7139.

[44] D. Vasilyev, E. Shirzadi, A. V. Rudnev, P. Broekmann, P. J. Dyson, *ACS Applied Energy Materials* **2018**, *1*, 5124-5128.

[45] D. V. Vasilyev, S. Shyshkanov, E. Shirzadi, S. A. Katsyuba, M. K. Nazeeruddin, P. J. Dyson, *ACS Applied Energy Materials* **2020**, *3*, 4690-4698.

[46] Y.-Y. Lee, D. Penley, A. Klemm, W. Dean, B. Gurkan, *ACS Sustainable Chemistry & Engineering* **2021**, *9*, 1090-1098.

[47] S. Dongare, O. K. Coskun, E. Cagli, K. Y. C. Lee, G. Rao, R. D. Britt, L. A. Berben, B. Gurkan, *ACS Catalysis* **2023**, *13*, 7812-7821.

[48] Y.-Y. Lee, K. Edgehouse, A. Klemm, H. Mao, E. Pentzer, B. Gurkan, *ACS Applied Materials & Interfaces* **2020**, *12*, 19184-19193.

[49] aX. Wei, X. Wen, Y. Liu, C. Chen, C. Xie, D. Wang, M. Qiu, N. He, P. Zhou, W. Chen, J. Cheng, H. Lin, J. Jia, X.-Z. Fu, S. Wang, *Journal of the American Chemical Society* **2022**, *144*, 11530-11535; bX. Zhu, X. Zhou, Y. Jing, Y. Li, *Nature Communications* **2021**, *12*, 4080.

[50] P. M. Krzywda, A. Paradelo Rodríguez, N. E. Benes, B. T. Mei, G. Mul, *Applied Catalysis B: Environmental* **2022**, *316*, 121512.

[51] M. Yuan, J. Chen, Y. Bai, Z. Liu, J. Zhang, T. Zhao, Q. Wang, S. Li, H. He, G. Zhang, *Angewandte Chemie International Edition* **2021**, *60*, 10910-10918.

[52] Y. Zhang, Y. Zhao, M. G. Sendeku, F. Li, J. Fang, Y. Wang, Z. Zhuang, Y. Kuang, B. Liu, X. Sun, *Small Methods* **2024**, *8*, 2300811.

[53] J. Li, N. Kornienko, *Chemical Science* **2022**, *13*, 3957-3964.

[54] Y. Wu, Z. Jiang, Z. Lin, Y. Liang, H. Wang, *Nature Sustainability* **2021**, *4*, 725-730.

[55] Z. Tao, Y. Wu, Z. Wu, B. Shang, C. Rooney, H. Wang, *Journal of Energy Chemistry* **2022**, *65*, 367-370.

[56] T. Supap, C. Saiwan, R. Idem, P. P. T. Tontiwachwuthikul, *Carbon Management* **2011**, *2*, 551-566.

[57] M. Li, M. N. Idros, Y. Wu, T. Burdyny, S. Garg, X. S. Zhao, G. Wang, T. E. Rufford, *Journal of Materials Chemistry A* **2021**, *9*, 19369-19409.

[58] K. Yang, R. Kas, W. A. Smith, T. Burdyny, *ACS Energy Letters* **2021**, *6*, 33-40.

[59] E. R. Cofell, U. O. Nwabara, S. S. Bhargava, D. E. Henckel, P. J. A. Kenis, *ACS Applied Materials & Interfaces* **2021**, *13*, 15132-15142.

[60] S. Subramanian, J. Middelkoop, T. Burdyny, *Sustainable Energy & Fuels* **2021**, *5*, 6040-6048.

[61] X. Wang, S. Zhang, J. Yao, H. Li, *Industrial & Engineering Chemistry Research* **2019**, *58*, 7352-7361.

[62] C. S. M. Kang, X. Zhang, D. R. MacFarlane, *The Journal of Physical Chemistry C* **2018**, *122*, 24550-24558.

[63] L. M. Galán Sánchez, G. W. Meindersma, A. B. de Haan, *Chemical Engineering Research and Design* **2007**, *85*, 31-39.

[64] J. Feng, K. Zhou, C. Liu, Q. Hu, H. Fang, H. Yang, C. He, *ACS Applied Materials & Interfaces* **2022**, *14*, 38717-38726.

[65] K. R. Seddon, A. Stark, M.-J. Torres, *Pure and Applied Chemistry* **2000**, *72*, 2275-2287.

[66] Y. Cao, Y. Chen, X. Sun, Z. Zhang, T. Mu, *Physical Chemistry Chemical Physics* **2012**, *14*, 12252-12262.

[67] S. Seo, M. Quiroz-Guzman, M. A. DeSilva, T. B. Lee, Y. Huang, B. F. Goodrich, W. F. Schneider, J. F. Brennecke, *The Journal of Physical Chemistry B* **2014**, *118*, 5740-5751.

[68] M. Liu, Y. Pang, B. Zhang, P. De Luna, O. Voznyy, J. Xu, X. Zheng, C. T. Dinh, F. Fan, C. Cao, F. P. G. de Arquer, T. S. Safaei, A. Mepham, A. Klinkova, E. Kumacheva, T. Filleter, D. Sinton, S. O. Kelley, E. H. Sargent, *Nature* **2016**, *537*, 382-386.

[69] S. Ringe, E. L. Clark, J. Resasco, A. Walton, B. Seger, A. T. Bell, K. Chan, *Energy & Environmental Science* **2019**, *12*, 3001-3014.

[70] A. K. Ummireddi, S. K. Sharma, R. G. S. Pala, *Catalysis Science & Technology* **2022**, *12*, 519-529.

[71] P. Zhan, J. Zhuang, S. Yang, X. Li, X. Chen, T. Wen, L. Lu, P. Qin, B. Han, *Angewandte Chemie International Edition*, *n/a*, e202409019.

[72] Y. Zhao, H. Zhou, X. Zhu, Y. Qu, C. Xiong, Z. Xue, Q. Zhang, X. Liu, F. Zhou, X. Mou, W. Wang, M. Chen, Y. Xiong, X. Lin, Y. Lin, W. Chen, H.-J. Wang, Z. Jiang, L. Zheng, T. Yao, J. Dong, S. Wei, W. Huang, L. Gu, J. Luo, Y. Li, Y. Wu, *Nature Catalysis* **2021**, *4*, 134-143.

[73] Y. Gao, J. Wang, Y. Yang, J. Wang, C. Zhang, X. Wang, J. Yao, *Nano-Micro Letters* **2023**, *15*, 158.

[74] aW. Qiu, S. Qin, Y. Li, N. Cao, W. Cui, Z. Zhang, Z. Zhuang, D. Wang, Y. Zhang, *Angewandte Chemie International Edition* **2024**, *63*, e202402684; bR. Casebolt, K. Levine, J. Suntivich, T. Hanrath, *Joule* **2021**, *5*, 1987-2026.

[75] C. S. Gerke, M. Klenk, P. Zapol, V. S. Thoi, *ACS Catalysis* **2023**, *13*, 14540-14547.

Entry for the Table of Contents

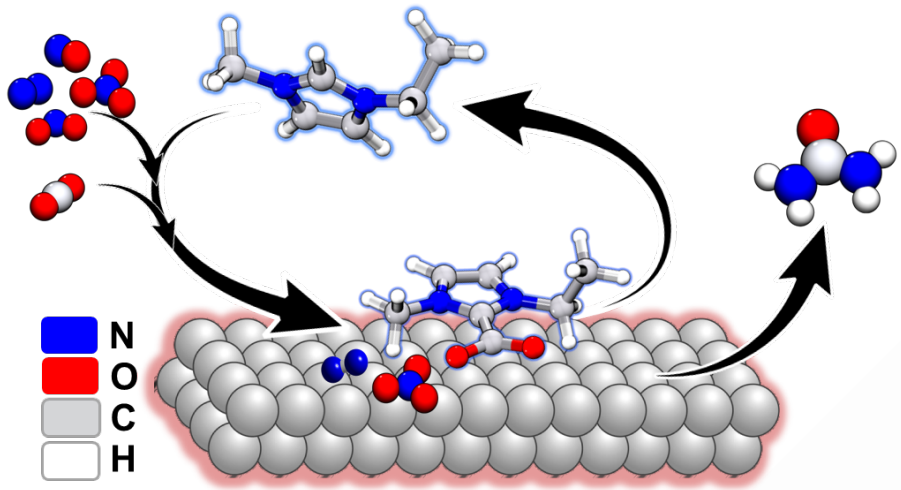

Formation of C–N bonds through co-electrolysis of CO_2 and nitrogen-containing compounds is a promising method for converting waste and readily available sources into valuable products such as urea – a nitrogen fertilizer. This paper presents the concept of utilizing ionic liquids (ILs) as electrolytes to leverage IL-enabled microenvironments to stabilize reaction intermediates at the electrode-electrolyte interface, thus promoting efficient C–N bond formation at reduced overpotentials.

Institute and/or researcher Twitter usernames: @saudagardongare; @CaseEngineer; @CWRU